Journal of Membrane Computing (2021) 3:35–50
https://doi.org/10.1007/s41965-020-00038-y

REGULAR PAPER

Modeling diel vertical migration with membrane computing

Manuel García-Quismondo[1,2] · William D. Hintz[2] · Matthew S. Schuler[2] · Rick A. Relyea[2]

Received: 7 February 2020 / Accepted: 25 March 2020 / Published online: 14 April 2020

Abstract
Diel vertical migration (DVM) is an important ecological phenomenon in which zooplankton migrate vertically to deal with trade-offs associated with greater food availability in shallow waters and lower predator risk in deep waters due to lower light availability. Because of these trade-offs, DVM dynamics are particularly sensitive to changes in light intensity at the water surface. Therefore, changes in the proportion of cloudy and sunny days have the potential to disrupt DVM dynamics. We propose a new membrane computing model that captures the effect of cloud cover on DVM in *Daphnia*, and we use it to explore the impacts of an increased proportion of cloudy days that are predicted to occur with climate change. Our 2-dimensional, spatially explicit model integrates multiple trophic levels from abiotic nutrients to *Daphnia* predators. We analyzed the effect that different proportions of cloudy and sunny days throughout the summer have on our model. The model simulations suggest that an increase in sunny days promotes a high phytoplankton concentration near the surface but does not necessarily promote an increased abundance of *Daphnia*. Our model also suggests that a higher proportion of cloudy days would increase *Daphnia* abundance due to a shift in the vertical distribution of *Daphnia* populations towards superficial waters. Our results highlight that climate changes in multiple regions will affect animal migrations leading to altered food web dynamics in freshwater ecosystems, and emphasize the potential of membrane computing as a modeling framework for spatially and temporally explicit ecological processes.

Keywords Diel vertical migration · Limnology · *Daphnia* · Mathematical modeling · Simulation · Population dynamics

1 Introduction

Climate change is affecting ecosystems worldwide, transforming habitats by altering the variability of weather conditions such as cloud cover [24]. Changing weather patterns can have widespread effects on animal behaviors including the migratory behaviors of birds and mammals [6, 43, 47, 67, 69]. A common form of animal migration in aquatic invertebrates is diel vertical migration (DVM), in which zooplankton migrate between deep and shallow waters. The mainstream hypothesis is that the purpose of DVM is to balance the decreased growth associated with lower phytoplankton concentrations in deep waters and the higher risk of predation associated with more phytoplankton-rich shallow waters [36, 41, 48, 50, 63].

Zooplankton tend to perform DVM when the benefits of obtaining food resources outweigh the costs associated with the perceived risk of predation [50, 63]. In addition to detecting food availability, zooplankton must detect predators; to do this, they rely on visual, mechanical and chemical cues (kairomones) [8, 10, 25, 26, 28, 36, 60]. In the case of the ubiquitous zooplankton *Daphnia*, DVM is principally regulated by ultraviolet radiation, with the concentration of kairomones in the water playing a secondary role [46, 70]. In this sense, Rose et al. [61] experimentally studied the effect of ultraviolet radiation and predator presence on DVM in *Daphnia*. They found a significant effect of ultraviolet radiation on the vertical distribution of *Daphnia*, with more individuals in deep waters at high levels of radiation than at low levels. Similar mesocosm experiments support the hypothesis that *Daphnia* remain in deeper waters in the presence

Electronic supplementary material The online version of this article (https://doi.org/10.1007/s41965-020-00038-y) contains supplementary material, which is available to authorized users.

✉ Manuel García-Quismondo
mgarciaquismondo@us.es

[1] Research Group on Natural Computing, University of Sevilla, ETS Ingeniería Informática. Av. Reina Mercedes, s/n, 41012 Sevilla, Spain

[2] Darrin Fresh Water Institute, Rensselaer Polytechnic Institute, 110 8th Street, 307 MRC, Troy, NY 12180, USA

of ultraviolet radiation [23, 30]. However, other factors like temperature and food concentration can also affect DVM, which should be considered in models that describe the drivers of DVM [39, 50].

Given the important role of ultraviolet radiation (which principally arrives at the water surface as part of the sunlight frequency spectrum) in driving DVM behavior in zooplankton, an interesting question is how DVM might be affected by variation in cloud cover. This variation in cloud cover is an expected consequence of a potential alteration of precipitation events [71]. Multiple computational bioenergetics models have been developed to analyze the effects of light intensity and food concentration of DVM in *Daphnia*. Such models have been based on partial differential equations (PDE) [9, 57, 58, 63], machine-learning frameworks [27], and individual-based dynamics [29, 59, 60]. Most models focus on capturing the dynamics of DVM for a particular scenario and analyze the simulation results under different conditions of light and food concentration. However, additional perspectives have also been explored. To automate the construction of DVM models based on sensor data, Eiane et al. [27] trained an artificial neural network using a genetic algorithm. In addition, Morozov et al. [51] and Samanta et al. [63, 64] analyzed the stability of various autonomous PDE-based models on DVM dynamics and obtained a set of theorems that characterize the conditions for equilibria.

Most publications on membrane computing [55] focus on aspects of theoretical computer science and computational complexity [17, 45, 49, 52, 65]. However, this paradigm is also an outstanding framework to capture the spatio-temporal aspects of population dynamics in many species by representing spatial regions as membranes [3, 7, 18–22, 31, 32, 34]. Nevertheless, the discrete nature of P systems makes it difficult to represent continuous quantities that are inherent to virtually any ecological process. Therefore, it is necessary to introduce features in P systems modeling population dynamics that are capable of representing and processing continuous values [31, 34]. To this end, we propose a model in which the transition steps between computations are defined both by object rewriting rules that capture the dynamics of groups of individuals and discrete-time equations that handle continuous values.

In this work, we propose a membrane computing model to analyze the role that the incidence of light intensity on the water surface has on *Daphnia* DVM. To our knowledge, our work is the first to address the effect of the annual proportion of cloudy days on *Daphnia* DVM behavior from the perspective of computational dynamical modeling and simulation. We consider three categories of light intensity: normal (i.e., days with typical summer light intensity), sunny (i.e., a higher proportion of sunny summer days), and cloudy (i.e., a lower proportion of sunny summer days). We focus our analysis on summertime dynamics, excluding wintertime when the surface of temperate lakes often freeze, causing most *Daphnia* to exist as resting eggs on the lake bottom. We hypothesized that a high proportion of cloudy days will shift the center of biomass of *Daphnia* towards the lake surface, shortening the distance between the center of biomass of *Daphnia* and phytoplankton. A high perceived risk of predation is expected to limit DVM and drive *Daphnia* to deep waters, where their development is impeded due to low temperatures and less abundant food (Fig. 1) [50]. In this scenario, the center of biomass of *Daphnia* and phytoplankton is expected to be large. We also hypothesize that the perceived risk of predation would be inversely correlated with *Daphnia* biomass, indicating that predator avoidance maximizes *Daphnia* abundance even though food is more scarce in deep waters that are safe from predation.

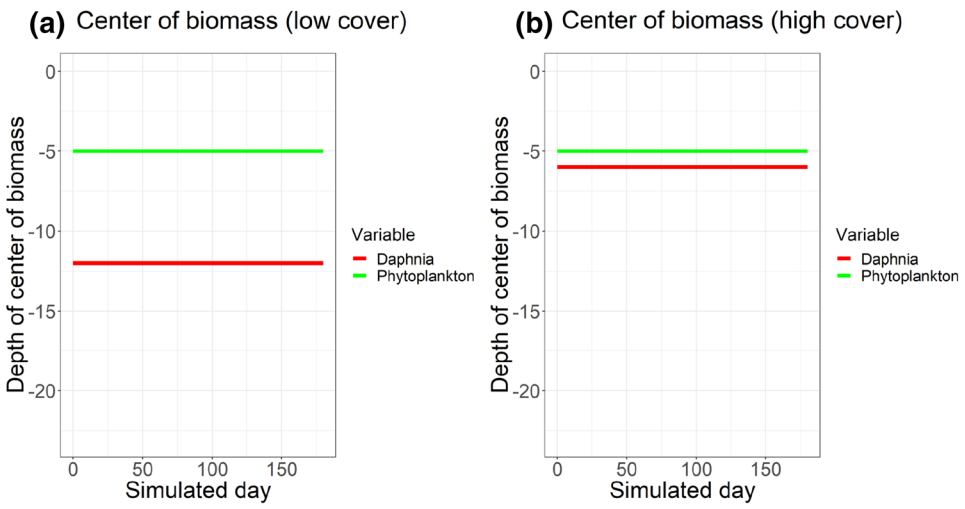

Fig. 1 Hypothesized depths of the centers of biomass of *Daphnia* and phytoplankton for low cloud cover (**a**) and high cloud cover (**b**)

2 Methods

We created a membrane computing model structured in three sets of object rewriting rules and discrete-time equations (modules), with each module capturing the dynamics of a trophic level (abiotic resources, phytoplankton and *Daphnia*). The membrane graph that defines the structure of a membrane computing model provides a natural manner to represent regions with different properties, and permits to express local phenomena in a straightforward way [18, 19, 33, 34]. In the case of the present model, membranes represent regions in a bidimensional space, and the adjacency between membranes in this graph encodes naturally the adjacency between spatial regions. Likewise, objects are a natural manner to encode discrete entities such as animals or groups of animals [3, 18, 19, 34].

The proposed model integrates aspects whose dynamics are captured using differential equations (such as light intensity and temperature), as well as others that are modeled using rewriting rules (e.g. phytoplankton development and *Daphnia* dynamics). Our model represents a 2D section of the lake of size depth × width, in which the depth of the lake is variable as a function of the water column. Abiotic resources (light intensity and nutrients) promote phytoplankton biomass. Light is in turn attenuated by phytoplankton, impeding photosynthesis in deep waters. Phytoplankton growth is modulated by abiotic resources, water temperature and a carrying capacity factor that curbs algae proliferation at large concentrations of phytoplankton biomass. The *Daphnia* lifecycle consists of egg, juvenile and adult development stages. Adult individuals lay eggs in function of their biomass. These eggs hatch into juveniles that, after a predefined number of hours, reach adulthood. Adult and juvenile individuals feed on phytoplankton, thus their biomass growth is modulated by phytoplankton biomass concentration plus a carrying capacity factor. Adult and juveniles migrate between shallow waters, where the concentration of phytoplankton is larger because of the higher light intensity, and deep waters, where they shelter from predators and harmful light intensity levels. The model mechanics are illustrated in Fig. 2.

Fig. 2 Conceptual diagram of model mechanics

2.1 Parameter calibration

The model parameters and their values are listed as supplementary material. We optimized the parameters of our model to maximize fitness with field data registers on *Daphnia* abundance, phytoplankton concentration, temperature, light intensity and nutrient concentration from the Jefferson Project at Lake George in NY, USA. Due to the sparsity of the data points and the variability in the temporal and spatial scales in the data (for instance, phytoplankton biomass was present as hourly average concentration through the water column in two different sites in the lake, while *Daphnia* abundance was calculated from monthly samples taken at specific depths), the use of this data for the numerical validation of the model is impractical.

2.2 Model description

The proposed model consists of a family of P systems defined as follows:

$\Pi = (H, G, T, \Theta, \Sigma, E, \mathcal{R}, D_0, \{\mathrm{ConcPh}(z, x, 0) \mid 0 \leq z \leq \mathrm{depth}_x, 1 \leq x \leq \mathrm{width}\}, \{I(0,0), \mathrm{Conc}_N(0), \mathrm{Conc}_P(0)\})$, where:

- H is a set of membranes representing the modeled lake $h_{z,x}, 0 \leq z \leq \mathrm{depth}_x, 1 \leq x \leq \mathrm{width}$, were depth_x is the depth of the lake at the water column x.
- $G = (V, S)$ is a graph on the membranes in H such as two membranes are adjacent if the vertical and horizontal distances between them is z_{diff} and x_{diff}, respectively, considering the vertical and horizontal distances between membranes $h_{z,x}$ and $h_{z',x'}$ as $|z - z'|$ and $|x - x'|$, respectively (Fig. 3).
- $T \geq 0$ is the simulation discrete time.
- $\Theta = \{L, P, F, E, M\}$ is an alphabet of configuration stages. These configuration stages represent abiotic resources, phytoplankton growth, *Daphnia* grazing (feeding), *Daphnia* laying eggs and *Daphnia* migrating, respectively. Each configuration is said to be in one of these stages, and the initial configuration is in stage L. To steer the non-deterministic semantics of P systems, rules can have an associated stage, meaning that they can only be applied on configurations in a given stage, and can set the stage of the next configuration. To denote that a rule is associated with a configuration stage, we add a superscript to the membrane in the left-hand side of the rule, and the stage of the next configuration is denoted as a superscript to the membrane in the right-hand side of the rule. As an example, $[a]^P \to [b]^F$, $a, b \in \Sigma$ denotes a rule associated with stage P that changes the configuration stage to F. Rules with no superscript on the left–hand side are not associated with any configuration stage and therefore can be applied on any configuration as long as the consumed objects exist, regardless of the stage of that configuration.
- Σ is an alphabet of symbols described as follows:
  - $D_{s_{i,t},num_{i,t},\mathrm{somat}_{i,t},\mathrm{gonad}_{i,t}}$, $0 \leq t \leq T$, $s_{i,t} \in \{J, A_k\}$, $\{0 \leq k \leq \mathrm{DTTA}\}$, $num_{i,t} \in \mathbf{N}^+$, $\mathrm{somat}_{i,t}, \mathrm{gonad}_{i,t} \in \mathcal{R}^+$ represent a *Daphnia* group i of $num_{i,t}$ individuals at instant t. $s_{i,t}$ represents the development stage of individuals in the group (J for Juvenile and A for Adult). *Daphnia* Time To Adulthood (DTTA) represents the number of hours passed since eggs hatch until juveniles become adults and are able to lay eggs. Likewise, $somat_{i,t}$ and $gonad_{i,t}$ represent the somatic (body) weight and gonad weight of the group. The incremental index $i, 0 \leq i \leq \#D$, where $\#D$ represents the total number of *Daphnia* and egg groups that ever existed during a given computation, is an identifier that is unique for the group, i.e., two *Daphnia* or egg groups with the same identifier i cannot coexist throughout the entire computation.
  - $\mathrm{Egg}_{l,\mathrm{eggn}}, 0 \leq l \leq \mathrm{DIT}$, $\mathrm{eggn} \in \mathbf{N}^+$ represent an egg group at instant t consisting of eggn eggs. *Daphnia* Incubation Time (DIT) represents the number of hours passed since eggs are laid until they hatch.
  - $Ph_{\mathrm{ConcPh}(z,x,t)}, 0 \leq t \leq T, \mathrm{ConcPh}(z, x, t) \in \mathcal{R}^+$ represent the concentration of phytoplankton at coordinates z, x and instant t.
  - $L_{I(0,t)}, 0 \leq t \leq T, I(0, t) \in \mathcal{R}^+$ represent light intensity at the water surface at instant t.
  - $N_{\mathrm{Conc}_N(t)}$, $P_{\mathrm{Conc}_P(t)}$, $\mathrm{Conc}_N(t)$, $\mathrm{Conc}_P(t) \in \mathcal{R}^+$ represent the concentration of nitrogen and phosphorus at instant t, respectively.
- E is a set of discrete-time equations that describe the relationships between the continuous quantities in the model. These equations are described for each one of the modules. It is important to highlight that the configuration of the model is encoded on the objects and their associated subindexes; the rest of the continuous variables in the model express continuous quantities in the modeled system and are not persistent.
- $\mathcal{R}$ is a set of rewriting rules that describe the dynamics of *Daphnia*, eggs and phytoplankton. These rules are described for each one of the modules.
- D_0 is a set of objects $D_{s_{i,0},\mathrm{num}_{i,0},\mathrm{somat}_{i,0},\mathrm{gonad}_{i,0}}$ that represent the i different groups of *Daphnia* in the system at the initial configuration. These groups are initially distributed across the membranes in H at random.

– $\{\text{ConcPh}(z,x,0) \mid 0 \le z \le \text{depth}_x, 1 \le x \le \text{width}\}$ represent the concentration of phytoplankton at the initial configuration of the system. Initially, each membrane in H contains an object $\text{Ph}_{\text{ConcPh}(z,x,0)}$.
– $\{I(0,0), \text{Conc}_N(0), \text{Conc}_P(0)\}$ represent light intensity at the water surface and concentration of nitrogen and phosphorus at instant 0. At the initial configuration, the top layer of membranes (e.g., membranes $h_{0,x}$, $1 \le x \le$ width) contains a copy of object $L_{I(0,0)}$, and each membrane in the system contains a copy of objects $N_{\text{Conc}_N(0)}$ and $P_{\text{Conc}_P(0)}$.

2.3 Module 1 – Abiotic resources

The first module captures the dynamics of the abiotic resources in the ecosystem (light intensity and nutrients), and is composed of the following equations.

2.3.1 Light intensity

We denote the light intensity at the lake surface (in watts/ m^2) at instant t as $I(0,t)$. Light intensity at depth z, water column x and instant t is denoted as $I(z,x,t)$, and is given by Eq. 1 [53, 62]:

$$I(z,x,t) = I(0,t) \times \exp(-lw \times I(0,t) \times \text{Att}(z,x,t)) \quad (1)$$

Here, lw denotes the steepness of the diffusion of light intensity across depths, and $\text{Att}(z,x,t)$ denotes the attenuation of light at depth z, water column x and instant t.

2.3.2 Light attenuation

Light attenuation at depth z, water column x and instant t is denoted as $\text{Att}(z,x,t)$ and is given by Eq. 2 [53]:

$$\text{Att}(z,x,t) = \left(\text{Turb} \times z + \text{AttCoff} \times \sum_{y=0}^{z} \text{ConcPh}(y,x,t) \right) \quad (2)$$

Attenuation is the sum of two components: $\text{Turb} \times z$, that represents water turbidity at depth z, and $\text{AttCoff} \times \sum_{y=0}^{z} \text{ConcPh}(y,x,t)$, that represents the attenuation due to accumulation of phytoplankton biomass at depth z, water column x and instant t. Here, Turb is the intrinsic turbidity of water, AttCoff is the attenuation coefficient of phytoplankton, and $\text{ConcPh}(y,x,t)$ is concentration of phytoplankton biomass at depth y, water column x and instant t.

2.3.3 Effect of light intensity on photosynthesis

The effect of light intensity on the photosynthetic activity of phytoplankton at a given depth z, water column x and instant t is modeled by Eq. 3 [53]:

$$\text{Lim}_{\text{Light}}(z,x,t) = \text{LightLim}_a \times (I(0,x,t) - I(z,x,t))/(\text{Att}(z,x,t) \times z_{\max}) \quad (3)$$

where $z_{\max}$ is the maximum depth in the modeled lake.

2.3.4 Effect of nutrients on photosynthesis

For the sake of simplification, the concentration of nutrients is assumed to be homogeneous across depths [68]. The effect of nutrient limitation on photosynthesis is modeled by Eq. 4 [72]:

$$\text{Lim}_{\text{Nut}}(t) = \text{NutLim}_a \times \text{Conc}_{\text{Nut}}(t)/(NutLim_b + \text{Conc}_{\text{Nut}}(t)) \quad (4)$$

with the values $\text{NutLim}_a = N\text{Lim}_a, \text{NutLim}_b = N\text{Lim}_b$ for nitrogen and $\text{NutLim}_a = PLim_a, \text{NutLim}_b = P\text{Lim}_b$ for phosphorus. To determine which nutrient (nitrogen or phosphorus) effectively limits photosynthesis, the ratio between the concentrations of nitrogen and phosphorus $\text{Conc}_N(t)/\text{Conc}_P(t)$ is calculated. If this ratio is greater or equal than a given constant Ratio_{NP}, then the limiting nutrient is phosphorus; otherwise, the limiting nutrient is nitrogen.

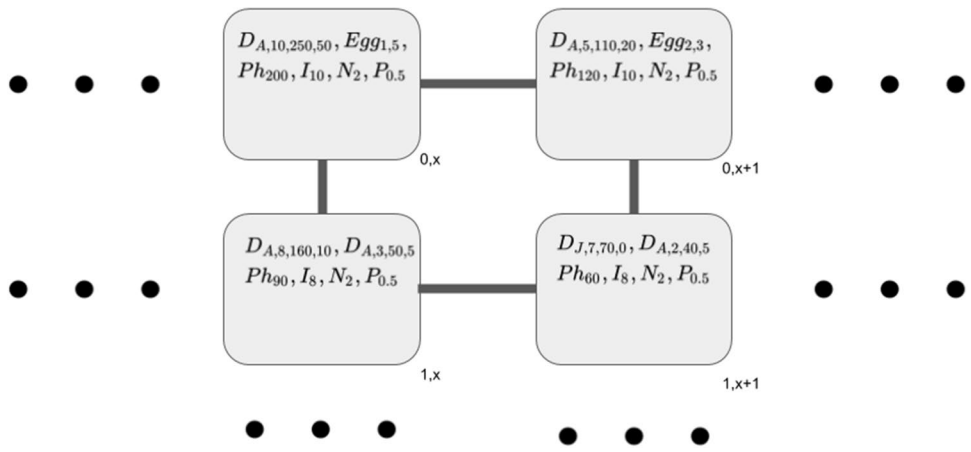

Fig. 3 Graphical representation of a section of the membrane graph G in a given configuration, including the objects described in Σ. Membranes $h_{0,x}$ represent the regions of the lake section at the water surface

2.3.5 Effect of water temperature on photosynthesis

The effect of water temperature on photosynthetic activity ($\mathrm{Lim}_{\mathrm{Temp}}(z,t)$) is calculated by Eq. 5 [53]:

$$\begin{aligned}\mathrm{Lim}_{\mathrm{Temp}}(z,t) = \exp(-(\mathrm{TOpt}-\mathrm{Temp}(z,t))^2/\mathrm{TSteepness}) \\ \times\ (1-1/(1+\exp(-\mathrm{Temp}(z,t)+\mathrm{TMax})))\end{aligned} \tag{5}$$

where $\mathrm{Temp}(z,t)$ represents the temperature at depth z and instant t (in Celsius degrees). Here, TOpt and TMax represent the optimal and maximum temperature values for photosynthesis. The term $\exp(-(\mathrm{TOpt}-\mathrm{Temp}(z,t))^2/\mathrm{TSteepness})$ is a Gaussian curve controlled by the steepness parameter TSteepness that peaks when the temperature is optimal, and the term $(1-1/1+\exp(-\mathrm{Temp}(z,t)+\mathrm{TMax}))$ is a sigmoidal function that increases the temperature penalty as the water temperature approaches the maximum tolerated temperature for phytoplankton. Therefore, photosynthetic activity reaches it maximum around the optimal temperature, and drops sharply as the maximum tolerated temperature is reached.

2.3.6 Update of abiotic resources

The following rules (6) update the values for light intensity on the water surface and concentrations of nitrogen and phosphorus at instant $t+1$, and enable rules associated with the configuration stage P to be applied:

$$[L_{I(0,t)}]^{L}_{z,x} \rightarrow [L_{I(0,t+1)}]^{P}_{z,x} \tag{6}$$

$$[\mathrm{Nut}_{\mathrm{Conc}_{\mathrm{Nut}}(t)}]^{L}_{z,x} \rightarrow [\mathrm{Nut}_{\mathrm{Conc}_{\mathrm{Nut}}(t+1)}]^{P}_{z,x}, \mathrm{Nut} \in \{N,P\} \tag{7}$$

2.4 Module 2: phytoplankton

The second module captures the dynamics of phytoplankton biomass. It is composed of the following equations.

2.4.1 Rate of photosynthetic activity

The rate of photosynthetic activity at depth z, water column x and instant t ($\mathrm{Photo}(z,x,t)$, in µg /(l × h)) is given by Eq. 8 [53]:

$$\begin{aligned}\mathrm{Photo}(z,x,t) = \mathrm{Lim}_{\mathrm{Nut}}(t) \times \mathrm{LightLim}(z,x,t) \\ \times\ \mathrm{Lim}_{\mathrm{Temp}}(z,t) \times\ \mathrm{ConcPh}(z,x,t)\end{aligned} \tag{8}$$

where $\mathrm{ConcPh}(z,x,t)$ is the concentration of phytoplankton biomass at depth z, water column x and instant t in µg /l, and $\mathrm{Lim}_{\mathrm{Temp}}(z,t)$ represents the effect of water temperature on photosynthetic activity.

2.4.2 Concentration of phytoplankton

The concentration of phytoplankton at depth z, water column x and instant $t+1$ ($\mathrm{Conc}(z,x,t+1)$, in µg/l) is calculated by Eq. 9:

$$\begin{aligned}\mathrm{ConcPh}_{\mathrm{noCC}}(z,x,t+1) &= (\mathrm{ConcPh}(z,x,t)+\mathrm{Photo}(z,x,t)-\mathrm{MortPh}(z,x,t)) \\ \mathrm{Graz}(z,x,t) &= \sum_i D\mathrm{Cons}_i(\mathrm{num}_{i,t}, s_{i,t}, z, x, t) \\ \mathrm{ConcPh}(z,x,t+1) &= \mathrm{CCPh}(z,x,t) \\ &\quad \times (\mathrm{ConcPh}_{\mathrm{noCC}}(z,x,t+1)-\mathrm{Graz}(z,x,t))\end{aligned} \tag{9}$$

Here, $\mathrm{ConcPh}_{\mathrm{noCC}}(z,x,t+1)$ (in µg /(l × h)) represents the concentration of phytoplankton before adjusting for carrying capacity and grazing, $\mathrm{Graz}(z,x,t)$ (in µg /(l × h)) represents the phytoplankton grazed by *Daphnia*, $D\mathrm{Cons}_i(\mathrm{num}_{i,t}, s_{i,t}, z, x, t)$ (in µg /(l × h)) represents the phytoplankton consumed by the *Daphnia* group i at instant t (described in Module 3), $\mathrm{MortPh}(z,x,t)$, (in µg /(l × h)) represents phytoplankton mortality as a function of nutrient concentration temperature and light intensity, and $\mathrm{CCPh}(z,x,t)$ represents the carrying capacity of phytoplankton. The concentration of phytoplankton at instant $t+1$ is updated as defined by Rule 10:

$$[\mathrm{Ph}_{\mathrm{ConcPh}(z,x,t)}]^{P}_{z,x} \rightarrow [\mathrm{Ph}_{\mathrm{ConcPh}(z,x,t+1)}]^{F}_{z,x}. \tag{10}$$

2.4.3 Phytoplankton mortality

Phytoplankton mortality at depth z, water column x and instant t ($\mathrm{MortPh}(z,x,t)$, in µg/(l × h)) is calculated by Eq. 11 [53]:

$$\begin{aligned}\mathrm{MortPh}(z,x,t) = \mathrm{IntMortPh} \times \mathrm{ConcPh}(z,x,t)/\mathrm{Lim}_{\mathrm{Nut}}(z,t) \\ \times\ \mathrm{Lim}_{\mathrm{Temp}}(z,t) \times \mathrm{Lim}_{\mathrm{Light}}(z,x,t)/I(0,x,t)\end{aligned} \tag{11}$$

Here, IntMortPh is the intrinsic mortality rate of phytoplankton. Phytoplankton mortality is directly proportional to the concentration of phytoplankton biomass ($\mathrm{ConcPh}(z,x,t)$), and is modulated by the effects of light intensity ($\mathrm{Lim}_{\mathrm{Light}}(z,x,t)/I(0,x,t)$), concentrations of nitrogen and phosphorus ($\mathrm{Lim}_{\mathrm{Nut}}(t)$) and temperature ($\mathrm{Lim}_{\mathrm{Temp}}(z,t)$) on the photosynthetic activity of phytoplankton.

2.4.4 Carrying capacity of phytoplankton

The effect of carrying capacity on the concentration of phytoplankton biomass at time t, water column x and depth z ($\mathrm{CCPh}(z,x,t)$) is calculated by Eq. 12:

$$\begin{aligned}\mathrm{CCPh}(z,x,t) = 1 - 1/(1 + \exp(-\mathrm{ConcPh}(z,x,t) \\ \times\ \mathrm{CCPhCoeff} + \mathrm{CCPhInt}))\end{aligned} \tag{12}$$

This equation is a sigmoidal function inversely proportional to the concentration of phytoplankton biomass ($\mathrm{PhConc}(z,x,t)$), and is modulated by the parameters CCPhCoeff and CCPhInt.

2.5 Module 3: *Daphnia*

The third module captures *Daphnia* dynamics and is divided into two submodules: *Daphnia* biomass and *Daphnia* migration. For computational simplicity, it is assumed that *Daphnia* aggregate into groups of individuals, modeling their dynamics in terms of groups. Therefore, in our model each object represents a group instead of an individual. It is important to note that more than one group can potentially coexist at the same depth z, water column x and instant t. *Daphnia* are assumed to transit through three development stages (egg, juvenile, and adult), and each group consists of individuals at the same development stage. Eggs are considered to be inactive (they do not filter water, lay eggs or die) until they hatch into juveniles; juveniles and adults consume phytoplankton, migrate and are subjected to mortality. Unlike adults, juveniles do not allocate gonad biomass (all their biomass is assumed to be somatic), do not lay eggs, and ultimately develop into adults if they survive to adulthood.

The biomass of a group consisting of $\mathrm{num}_{i,t}$ *Daphnia* individuals at development stage $s_{i,t}$, depth z, water column x and instant $t+1$ ($\mathrm{DBio}(\mathrm{num}_{i,t}, s_{i,t}, z, x, t)$, in µg/h) is modeled by Eq. 13:

$$\begin{aligned}&\mathrm{DBio}(\mathrm{num}_{i,t}, s_{i,t}, z, x, t+1) \\ &\quad = \mathrm{DBio}(\mathrm{num}_{i,t}, s_{i,t}, z, x, t) + (\mathrm{DCons}(\mathrm{num}_{i,t}, s_{i,t}, z, x, t) \\ &\quad - \mathrm{DBioLoss}(\mathrm{num}_{i,t}, s_{i,t}, z, x, t)) \times \mathrm{CCD}(\mathrm{num}_{i,t}, s_{i,t}, z, x, t)\end{aligned} \tag{13}$$

where $\mathrm{DBioLoss}(\mathrm{num}_{i,t}, s_{i,t}, z, x, t)$ represents the biomass lost on this group of $\mathrm{num}_{i,t}$ *Daphnia* individuals before adjusting for carrying capacity, $\mathrm{DCons}(\mathrm{num}_{i,t}, s_{i,t}, z, x, t)$ represents the amount of phytoplankton biomass (in µg) consumed by this group, and $\mathrm{CCD}(\mathrm{num}_{i,t}, s_{i,t}, z, x, t)$ represents the carrying capacity factor that limits the growth of *Daphnia* biomass.

2.5.1 Daphnia consumption

The amount of phytoplankton biomass consumed by a group of $\mathrm{num}_{i,t}$ *Daphnia* individuals on development stage $s_{i,t}$ at depth z, water column x and instant t per hour ($\mathrm{DCons}(\mathrm{num}_{i,t}, s_{i,t}, z, x, t)$, in µg/l) is defined in Eq. 14.

$$\begin{aligned}\mathrm{DCons}(\mathrm{num}_{i,t}, s_{i,t}, z, x, t) = \mathrm{DFilt}(s_{i,t}) \times \mathrm{ConcPh}(z,x,t) \\ \times\ \mathrm{num}_{i,t}/1000\end{aligned} \tag{14}$$

$\mathrm{DFilt}(s_{i,t})$ represents the filtering rate per individual in ml/(individual×h), and $\mathrm{PhConc}(z,x,t)$ represents the concentration of phytoplankton biomass in µg/l. Therefore, it is necessary to apply a conversion factor of 1000 ml/l. $\mathrm{DFilt}(s_{i,t})$ is calculated by Eq. 15 [11]:

$$\mathrm{DFilt}(s_{i,t}) = \mathrm{DFiltCoeff} \times \mathrm{DLength}(s_{i,t})^{\mathrm{DFiltExp}}. \tag{15}$$

This expression is modulated by the parameters DFiltCoeff and DFiltExp, and $\mathrm{DLength}(s_{i,t})$ represents expected the body length (in millimeters) of *Daphnia* on development stage $s_{i,t}$. The expected body length of a *Daphnia* individual at development stage $s_{i,t}$ is calculated by Eq. 16 [11]:

$$\mathrm{DLength}(s_{i,t}) = (\mathrm{DWeight}_{s_{i,t}}/\mathrm{DLengthCoeff})^{\mathrm{DLengthExp}} \tag{16}$$

where $\mathrm{DWeight}_{s_{i,t}}$ is the expected weight of *Daphnia* individuals in development stage $s_{i,t}$ (in grams) and DLengthCoeff and DLengthExp are coefficients that modulate the relationship between *Daphnia* weight and length.

For a group of $num_{i,t}$ *Daphnia* individuals at development stage $s_{i,t}$ at depth z, water column x and instant t, biomass is divided into somatic biomass($\mathrm{DSomBio}(\mathrm{num}_{i,t}, s_{i,t}, z, x, t)$, body weight) and gonad biomass (egg weight, $\mathrm{DGonBio}(\mathrm{num}_{i,t}, z, x, t)$ for adults and 0 for juveniles). Both are expressed in µg/l. Somatic biomass is defined in Eq. 17 (for juveniles) and Eq. 18 (for adults).

$$\begin{aligned}&\mathrm{DSomBio}(\mathrm{num}_{i,t}, J_k, z, x, t) = \mathrm{DCons}(\mathrm{num}_{i,t}, J_k, z, x, t), 0 \\ &\quad \le k \le \mathrm{DTTA}\end{aligned} \tag{17}$$

$$\begin{aligned}&\mathrm{DSomBio}(\mathrm{num}_{i,t}, A, z, x, t) = \mathrm{DCons}(\mathrm{num}_{i,t}, A, z, x, t) \\ &\quad - \mathrm{DGonBio}(\mathrm{num}_{i,t}, z, x, t)\end{aligned} \tag{18}$$

$$\begin{aligned}&\mathrm{DGonBio}(\mathrm{num}_{i,t}, z, x, t) = \mathrm{DCons}(\mathrm{num}_{i,t}, A, z, x, t) \times \\ &\quad \min(\mathrm{DGonProp}_{\max}, \max(0, \mathrm{ConcPh}(z,x,t) \times \mathrm{GonPropBiomass}))\end{aligned} \tag{19}$$

GonPropBiomass is a scaling factor and $\mathrm{DGonProp}_{\max}$ is the maximum possible proportion of biomass allocated to gonad weight. This expression is directly proportional to the concentration of phytoplankton biomass ($\mathrm{ConcPh}(z,x,t)$), and is limited by the parameter $\mathrm{DGonProp}_{\max}$. It is important to remark that the semantics of this rule is cumulative, i.e., if multiple groups of *Daphnia* are present in membrane (z, x) at instant t, all of them will graze $\mathrm{Ph}_{\mathrm{ConcPh}(z,x,t)}$, and $\mathrm{ConcPh}(z,x,t)$ will be decremented with each interaction. Therefore, *Daphnia* grazing is captured by Rule 20:

$$[D_{s_{i,t},num_{i,t},\text{somat}_{i,t},\text{gonad}_{i,t}}, \text{Ph}_{\text{ConcPh}(z,x,t)}]^F_{z,x} \rightarrow$$
$$[D_{s_{i,t},\text{num}_{i,t},somat_{i,t}+\text{DSomBio}(\text{num}_{i,t},s_{i,t},z,x,t),\text{gonad}_{i,t}+\text{DGonBio}(\text{num}_{i,t},s_{i,t},z,x,t)},$$
$$\text{Ph}_{\text{ConcPh}(z,x,t)-\text{DCons}(\text{num}_{i,t},s_{i,t},z,x,t)}]^E_{z,x} \tag{20}$$

2.5.2 Daphnia biomass loss

The amount of biomass lost by a group of $\text{num}_{i,t}$ *Daphnia* individuals at development stage $s_{i,t}$ and located at depth z, water column x and instant t per hour ($\text{DBioLoss}(\text{num}_{i,t}, s_{i,t}, z, x, t)$) is calculated by Eq. 21:

$$\begin{aligned}\text{DBioLoss}(\text{num}_{i,t}, s_{i,t}, z, x, t) &= \text{DMort} \times \text{DCons}(\text{num}_{i,t}, s_{i,t}, z, x, t) \\ &- \text{DStarv}(\text{num}_{i,t}, s_{i,t}, z, x, t) - \text{DPredRatio}(z, x, t) \\ &\times \text{DBio}(\text{num}_{i,t}, s_{i,t}, z, x, t)\end{aligned} \tag{21}$$

Here, $\text{DCons}(\text{num}_{i,t}, s_{i,t}, z, x, t)$ represents the amount of phytoplankton biomass (in µg) consumed by a group consisting of $\text{num}_{i,t}$ *Daphnia* individuals at development stage $s_{i,t}$ and located at depth z, water column x and instant t per hour, DMort represents the proportion of *Daphnia* biomass lost to natural mortality, $\text{DStarv}(\text{num}_{i,t}, s_{i,t}, z, x, t)$ represents *Daphnia* biomass lost to starvation per hour in µg/h and $\text{DPredRatio}(z, x, t)$ represents the proportion of *Daphnia* biomass lost to predation per hour in µg/h as a function predator biomass.

$\text{DStarv}(\text{num}_{i,t}, s_{i,t}, z, x, t)$ is calculated by Eq. 22:

$$\begin{aligned}\text{DStarv}(\text{num}_{i,t}, s_{i,t}, z, x, t) &= \text{DStarv} \times \text{num}_{i,t} \\ &\times \text{DWeight}_{s_{i,t}} / \text{PhConc}(z, x, t)\end{aligned} \tag{22}$$

where DStarv is a weight that modulates *Daphnia* starvation and $\text{DWeight}_{s_{i,t}}$ represents the expected weight of a *Daphnia* individual at stage *st*. Likewise, $\text{DPredRatio}(z, x, t)$ is calculated by Eqn. 23:

$$\text{DPredRatio}(z, x, t) = \text{DPredRatio} \times \text{PredBio}(z, x, t) \tag{23}$$

where DPredRatio is a weight that modulates predation of *Daphnia* directly proportional to predator biomass ($\text{PredBio}(z, x, t)$).

2.5.3 Daphnia carrying capacity

The effect of carrying capacity on *Daphnia* biomass is calculated by Eq. 24:

$$\begin{aligned}\text{CCD}(\text{num}_{i,t}, s_{i,t}, z, x, t) &= 1 - 1/(1 + \exp(-\text{DCons}(\text{num}_{i,t}, s_{i,t}, z, x, t) \\ &\times \text{CCDCoeff} + \text{CCDInt}))\end{aligned} \tag{24}$$

This sigmoidal function is modulated by the parameters CCDCoeff and CCDInt, and is analogous to the expression modeling carrying capacity in phytoplankton (Eq. 12).

2.5.4 Individual *Daphnia* in a group

Given a group of $\text{num}_{i,t}$ *Daphnia* individuals at development stage $s_{i,t}$ and at depth z, water column x and instant t, the number of individuals in this group at instant $t + 1$ ($\text{num}_{i,t+1}$) is calculated by Eq. 25:

$$\text{num}_{i,t+1} = \text{num}_{i,t} - \text{DBioLoss}(\text{num}_{i,t}, s_{i,t}, z, x, t)/\text{DWeight}_{s_{i,t}} \tag{25}$$

where $\text{DBioLoss}(\text{num}_{i,t}, s_{i,t}, z, x, t)$ is the biomass lost by this group at instant t and $\text{DWeight}_{s_{i,t}}$ is the expected weight of each *Daphnia* individual at stage $s_{i,t}$. In this case, / represents the integer division. Since this number decreases over time, the number of *Daphnia* individuals in a group tends to 0, and the generational replacement of individuals in the system is implemented through new groups of juveniles that hatch from eggs and reach adulthood.

2.5.5 Daphnia eggs laid by a group

Daphnia groups of adults lay eggs that, in turn, hatch into juvenile and eventually develop into adult individuals. The number of eggs laid by a group of $\text{num}_{i,t}$ *Daphnia* adults at depth z, water column x and instant t is calculated by Eqn. 26:

$$\begin{aligned}&\text{DEgg}(\text{num}_{i,t}, z, x, t) = \text{DGonBio}(num_{i,t}, A, z, x, t)/\text{DEggWeight} \\ &[D_{A,\text{num}_{i,t},\text{somat}_{i,t},\text{gonad}_{i,t}}]^E_{z,x} \rightarrow [D_{A,\text{num}_{i,t},\text{somat}_{i,t},\text{gonad}_{i,t}-\text{DEgg}(\text{num}_{i,t},z,x,t)}, \\ &\text{Egg}_{0,\text{DEgg}(\text{num}_{i,t},z,x,t)}]^M_{z,x}\end{aligned} \tag{26}$$

where $\text{DGonBio}(\text{num}_{i,t}, z, x, t)$ is the amount of *Daphnia* gonad biomass in the group and DEggWeight is the expected weight of each *Daphnia* egg. After DIT (for *Daphnia* Incubation Time) hours, these eggs hatch and give place to a new group of $N = \text{DEgg}(\text{num}_{i,t}, z, x, t)$ *Daphnia* juveniles, as shown in Rules 27 and 28.

$$[\text{Egg}_{l,\text{DEgg}(\text{num}_{i,t},z,x,t)}]_{z,x} \rightarrow [\text{Egg}_{l+1,\text{DEgg}(\text{num}_{i,t},z,x,t)}]_{z,x}, 0 \leq l \leq \text{DIT} \tag{27}$$

$$[\text{Egg}_{\text{DIT},\text{DEgg}(\text{num}_{i,t},z,x,t)}]_{z,x} \rightarrow [D_{J_0,num_{i,t},\text{DEggWeight}\times num_{i,t},0}]_{z,x} \tag{28}$$

Likewise, after DTTA (for *Daphnia* Time To Adulthood) hours, these individuals become adults and are able to allocate gonad biomass and, consequently, lay eggs, as shown in Rules 29 and 30:

$$[D_{J_k,num_{i,t},\text{DEggWeight}\times num_{i,t},0}]_{z,x} \rightarrow [D_{J_{k+1},num_{i,t},\text{DEggWeight}\times num_{i,t},0}]_{z,x} \quad 0 \leq k \leq \text{DTTA} \tag{29}$$

$$[D_{\text{DTTA},\text{num}_{i,t},\text{DEggWeight}\times num_{i,t},0}]_{z,x} \rightarrow [D_{A,\text{num}_{i,t},\text{DEggWeight}\times num_{i,t},0}]_{z,x} \tag{30}$$

2.5.6 *Daphnia* migration dynamics

The dynamics of *Daphnia* migration are captured as follows. Each group of *Daphnia* individuals at Membrane $h_{z,x}$ explores its vicinity at maximum horizontal and vertical distances of x_{diff} and z_{diff} (in meters). Each membrane $h_{z',x'}$ in this vicinity is a candidate membrane. If the candidate membrane has a light intensity value lower or equal than $I_{\text{max tolerable}}$ and a perceived risk of predation (calculated as $\text{PredBio}(z,x,t) \times I(z,x,t)$) lower or equal than PRP_{max} at instant t, then it is a viable candidate membrane, and the *Daphnia* group will migrate into the assessed membrane with a probability calculated by Eq. 31:

$$\text{PM}(z,x,z',x',t) = \exp(-\log(0.5) \times (\text{PhConc}(z,x,t) - \text{PhConc}(z',x',t))/\text{PhConcExpDiff}) \tag{31}$$

where log is the natural logarithm, $\text{PhConc}(z,x,t)$ and $\text{PhConc}(z',x',t)$ are the concentrations of phytoplankton biomass in $h_{z,x}$ and $h_{z',x'}$, and PhConcExpDiff is a parameter that represents the expected value of the difference between the phytoplankton concentrations in two membranes. Therefore, when the difference between concentrations of phytoplankton biomass is equal to the expected value, the probability of migration is equal to 0.5. If the *Daphnia* group migrates to the candidate membrane, a random sample of not yet assessed membranes in the vicinity are explored.

To capture the semantics of migration dynamics, Rule 32 is applied with probability $\text{PM}(z,x,z',x',t)$:

$$[D_{s_{i,t},\text{num}_{i,t},\text{somat}_{i,t},\text{gonad}_{i,t}}]^M_{z,x} \rightarrow [D_{s_{i,t},\text{num}_{i,t},\text{somat}_{i,t},\text{gonad}_{i,t}}]^L_{z',x'} \tag{32}$$

3 Results

We implemented a simulator for this model in C++, and simulated the model for 2 years on a Sun Grid Engine (SGE) cluster. The area simulated was a section of the lake with maximum depth of 23 m across all water columns, and the simulations were executed with a spatial resolution of 1 m (that is to say, each membrane represents a 1 m × 1 m area) and a temporal resolution of 1 h.

3.1 Linear mixed effect analysis

To explore the effects that the perceived predation risk (PRP_{max}) and the proportion of cloudy days throughout the summer ($\text{Prop}_{\text{cloud}}$) have on the average depth of the center of biomass of *Daphnia* over time ($\text{ADB}_{\text{Daphnia}}$), we built a set of linear mixed effect models using the *nlme* package [54] in R [56]. Since our model focuses on *Daphnia* migration dynamics, we only considered adult and juvenile individuals for the calculations of *Daphnia* abundance and center of biomass, leaving eggs aside. In addition, egg biomass is not significant in our model in comparison with biomass from adult and juvenile individuals, thus omitting eggs does not significantly change biomass computations. For each response variable analyzed, we built two different linear models; first, we fixed perceived predation risk (PRP_{max}) and varied the proportion of cloudy days ($\text{Prop}_{\text{cloud}}$). Then, we swapped the fixed and random variables. Predation risk in *Daphnia* varied between null avoidance of predators (0), in which *Daphnia* solely maximizes food availability, and maximum avoidance of predators (1), in which *Daphnia* avoid predators at all costs. Likewise, the proportion of cloudy days throughout the year varied from 0 to 1. Using these models, we analyzed the role of these variables on the mean biomass of *Daphnia* and their average depth over time.

We also built a set of linear mixed effect models to analyze the role of phytoplankton concentration on the mean biomass of *Daphnia* and their average depth over time. These models are grouped in two sets. In the first set of models, the concentration of phytoplankton biomass was fixed. In the second set of models, the depth of the center of biomass of phytoplankton was fixed. In our model, the concentration of phytoplankton biomass is highly dependent on the light intensity at the surface. Therefore, in these models the random variable was set to PRP_{max} and not to $\text{Prop}_{\text{cloud}}$ to maintain the assumption of independence between variables.

3.2 Analysis results

We observed that predation risk (PRP_{max}) impedes *Daphnia* from migrating to shallow waters, independent of the cloud cover. For low values of predation risk (0.01), *Daphnia* migrate regularly to the surface in search for food. On the contrary, for medium and high values of predation risk (0.41–1.00) *Daphnia* remain in deep waters (deeper than 10 m) and rarely migrate to the surface. In contrast, the center of biomass of phytoplankton remains at a similar depth in both scenarios. The difference between these centers of biomass causes a lower abundance of *Daphnia* than in the high cloud cover scenario, where the overall phytoplankton

biomass is lower but shallow waters are more accessible to *Daphnia* (Fig. 4).

We also observed that *Daphnia* tend to migrate to deep waters in scenarios with low cloud cover. For the models where the proportion of cloudy days throughout the summer is fixed ($Prop_{cloud}$), our analysis indicates an inverse correlation between $Prop_{cloud}$ and the average depth of the center of *Daphnia* biomass ($ADB_{Daphnia}$) ($p < 0.001$). Specifically, the depth of the center of *Daphnia* biomass is 9.8 m for $Prop_{cloud} = -0.8$; this decreases to 8.1 m for $Prop_{cloud} = 0.8$. Our analysis also indicates a direct correlation between $Prop_{cloud}$ and the average abundance of *Daphnia* biomass over time ($AAB_{Daphnia}$) ($p < 0.001$). As the proportion of cloudy days rises, the increase in the abundance of *Daphnia* biomass is dramatic, going from 4.2 µg/l for 80% of sunny days to 13.65 µg/l for 80% of cloudy days (3.23-fold increase). These results suggest that, perhaps counterintuitively, *Daphnia* are more abundant in scenarios with a large proportion of cloudy days throughout the summer. The reason is that a higher proportion of sunny days causes *Daphnia* to avoid shallow waters due to increased predation risk, despite the fact that these conditions produce the highest concentration of phytoplankton biomass.

However, our linear analysis of the model simulations indicates that the main factor driving DVM dynamics is perceived predation risk (PRP_{max}). This analysis suggests a close direct correlation between perceived predation risk and the average depth of *Daphnia* over time ($ADB_{Daphnia}$) ($p < 0.001$). The estimated depth of the center of *Daphnia* biomass is 5.8 m for $PRP_{max} = 0.01$ and 12.1 m, for $PRP_{max} = 0.41$ (i.e., a 2.07-fold increase). Likewise, the analysis yields a negative correlation between perceived predation risk PRP_{max} and average abundance of biomass of *Daphnia* over time ($AAB_{Daphnia}$) ($p < 0.001$). The concentration values range from 11.7 µg/l for $PRP_{max} = 0.01$ to 6.69 µg/l for $PRP_{max} = 0.41$ (i.e., a 1.76-fold increase). These results suggest that, in our model, the proportion of cloudy days throughout the summer, although relevant, plays a secondary role in *Daphnia* DVM dynamics and that predation risk is the main factor that drives this behavior. Finally, we also observed that a high concentration of food is not necessarily correlated with a large abundance of *Daphnia*. The results also indicate that the average concentration of phytoplankton biomass over time (ACB_{phyto}) is inversely correlated with average abundance of *Daphnia* biomass over time (AAB_{phyto}) ($p < 0.001$). In our simulations, the average abundance of *Daphnia* biomass varies from 12.3 µg/l when ACB_{phyto} is 100 µg/l to 3.35 µ g/l when ACB_{phyto} is 164 µg/l (i.e., a 3.68-fold decrease). To complement this analysis, we also measured the statistical significance of the inverse correlation between phytoplankton biomass and proportion of cloudy days throughout the year. The model indicates a strong direct correlation between the depth of the center of phytoplankton biomass and the depth of the center of *Daphnia* biomass ($p < 0.001$). The values for $ADB_{Daphnia}$ range from 8.1 m when the average depth of the center of phytoplankton biomass is 0.03–10.4 m when the average depth of the center of phytoplankton biomass is 1.23 m (1.3-fold increase). In combination, these results suggest that cloud cover is possibly the main factor that drives abundance of phytoplankton. At the same time, larger values of phytoplankton biomass do not imply larger values of *Daphnia* abundance. One possible hypothesis is that low values of cloud cover promote phytoplankton growth, but at the same time, they reveal the presence of predators, which scare *Daphnia* away from the water surface where the concentration of phytoplankton biomass is higher. Therefore, *Daphnia* does not benefit from this increase in its food resources. The relationships between these variables are graphically represented in Fig. 5.

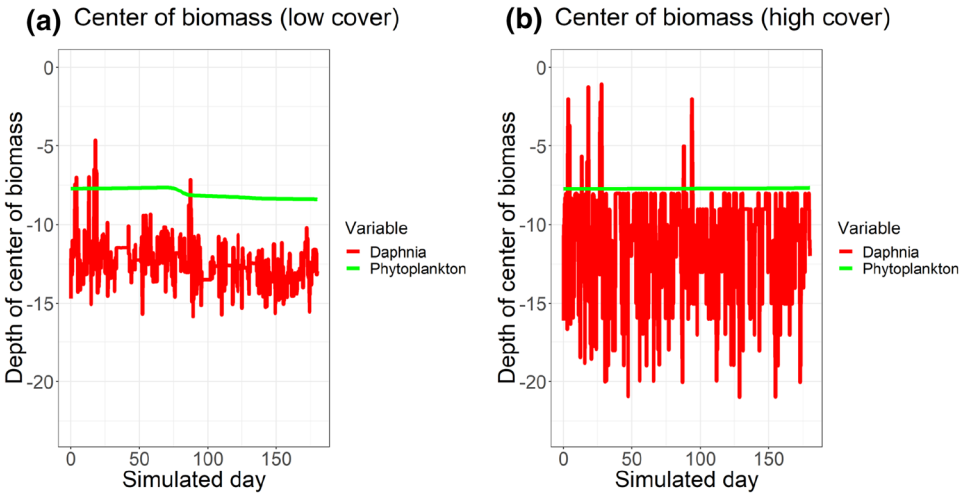

Fig. 4 Model predictions for the depth of the centers of biomass of *Daphnia* (red) and phytoplankton (green). **a** A scenario with low cloud cover. **b** A scenario with high cloud cover

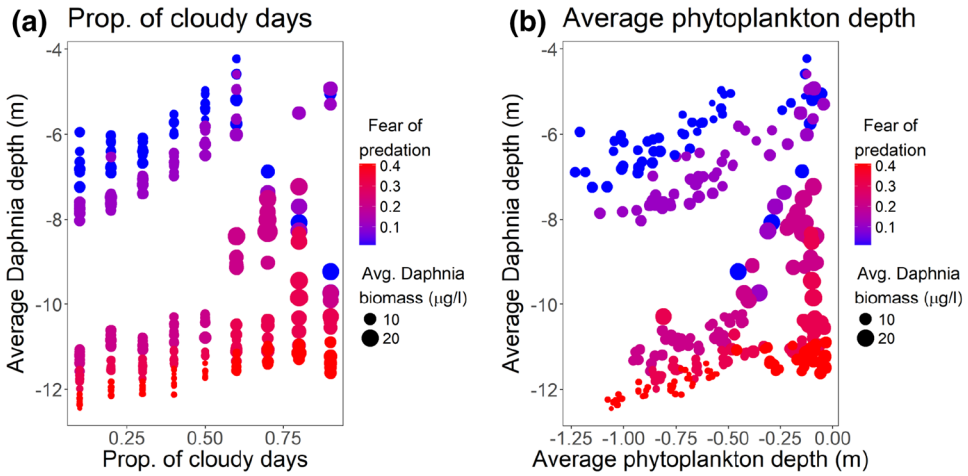

Fig. 5 Effect of different input variables in the model (*x*-axis) on the depth of the center of biomass of *Daphnia* (*y*-axis) and on *Daphnia* biomass (point size). **a** Effect of the proportion of cloudy days. **b** Effect of the depth of the center of biomass of phytoplankton

4 Discussion

The impact of climate change on DVM is a growing area of research. However, the limited capacity to modulate and observe the behavior of animals in experiments and field studies necessitates computational dynamical models to examine patterns and processes at scales difficult to elucidate by any single or series of studies. One of the principal manners by which climate change could influence DVM dynamics and the distribution of zooplankton across depths is by altering the proportion of cloudy versus sunny days throughout the year due to altered precipitation patterns.

Membrane computing is an exceptional framework to capture the spatial dynamics of population dynamics, and its discrete nature permits to model groups of individuals as objects that interact among each other and with a spatially-discrete environment and migrate across it. These properties make this computational framework an excellent candidate to model DVM. However, continuous quantities appear on virtually any ecological process, and DVM is not an exception. Thus, to capture the dynamics of DVM by simulating computations of a membrane computing model, it is necessary to include features capable of manipulating continuous variables such as light intensity, somatic and gonad weight, abiotic nutrient concentration and algae biomass. In this sense, we propose a membrane computing model with discrete-time equations to capture both the discrete and continuous aspects of DVM.

Our model confirms our a-priori hypothesis that a high proportion of cloudy days drives *Daphnia* to shallow waters, whereas a high proportion of sunny days drives *Daphnia* to deep waters. This result supports the observed effect of light intensity on the distribution of *Daphnia* biomass across depths in in vivo experiments. In particular, the analysis of our model simulations supports the observation that a low annual light intensity at the surface is correlated with a high proportion of *Daphnia* individuals in shallow waters [40, 44, 61]. Likewise, our results are consistent with the observation that climatological events that dramatically diminish light intensity at the surface (such as storms and heavy rainfall) provoke substantial shifts on the vertical distribution of *Daphnia* towards shallow waters [61].

Our model contradicts the a-priori hypothesis that a high proportion of cloudy days would reduce *Daphnia* population numbers because of the lower photosynthetic activity and, therefore, lower phytoplankton concentrations. One explanation is that high cloud cover levels impede the visual detection of predators and decrease the perceived risk of predation, encouraging *Daphnia* to migrate to shallow waters in search for high phytoplankton concentrations. This result is not consistent with the experimental observations that suggest that lower cloud cover levels enable the development of larger populations of *Daphnia* through larger phytoplankton concentrations and better visual perception of predators [23, 30, 61]. However, these works were limited to low phytoplankton concentrations, and do not cover the case in which food is not a constant limiting factor for *Daphnia* populations.

Our results suggest that the strategy of maximizing food intake yields larger *Daphnia* populations as opposed to the strategy of minimizing the risk of predation. Support for this was a direct correlation between the proportion of cloudy days and the abundance of *Daphnia* combined with the negative correlation between the perception of risk of predation and the abundance of *Daphnia*. This suggests that the impact of predation on *Daphnia* biomass is low in comparison with other elements in the system, such as food concentration and light intensity. Hansson and Hylander [40] obtained similar results when they observed that ultraviolet radiation is the major force that drives the vertical distribution of *Daphnia*, and the addition of different regimes of predator abundance does not change this distribution significantly.

The model simulations suggest that phytoplankton concentration is inversely correlated with *Daphnia* abundance.

This contradicted our a-priori hypothesis that a high concentration of food should imply a high abundance of *Daphnia*. Given that there exists a strong inverse correlation between phytoplankton concentration and proportion of cloudy days throughout the year, one explanation is that a low cloud cover promotes photosynthetic activity, which results in a high phytoplankton concentration. However, at the same time these low cloud cover levels drive *Daphnia* to deep waters, where phytoplankton concentration is lower. This result complements the aforementioned positive correlation between annual proportion of cloudy days and *Daphnia* abundance, and highlights one of the main assets of our model: the real-time interaction between phytoplankton dynamics and light intensity. Less surprisingly, the model analysis suggests a strong direct correlation between the depth of the centers of biomass of phytoplankton and *Daphnia*. This indicates that *Daphnia* actively migrate across depths in search for regions with high phytoplankton concentrations.

5 Conclusions

Climate change is disrupting animal migratory behaviors around the globe. Diel vertical migration (DVM) is an important process where aquatic invertebrates migrate between deep and shallow waters maximizing food consumption and minimizing predation exposure. Here, we present the first computational dynamical model that explicitly addresses the effects of climatic change in the annual proportion of cloudy days on DVM dynamics in *Daphnia*. We selected membrane computing to model DVM because its discrete nature permits to easily represent groups of animals that migrate and interact with the environment and with each other, and include discrete-time equations to update the continuous quantities inherent to DVM throughout the model computations. Due to climate change, the frequency of drought conditions is increasing in some regions, and in others, precipitation events are becoming more frequent [24]. Our model suggests that disruptions in the annual proportion of cloudy and sunny days due to changes in precipitation events will interact with natural stressors like predation risk and alter DVM dynamics. We found that high primary productivity will be associated with a higher biomass of *Daphnia* in years with more cloudy days. However, in regions that are becoming more arid or experiencing a higher frequency of drought conditions, the lack of cloudy days or precipitation may cause a spatial separation between *Daphnia* grazers and their food resources. Predation risk will magnify the disconnection between *Daphnia* grazers and phytoplankton resources in regions that experience fewer precipitation events. Importantly, our results highlight that interactions between climate change and predation have the potential to dramatically disrupt food web dynamics due to changes in DVM in *Daphnia* zooplankton.

6 Future work

The current version of our model is 2-dimensional. This characteristic limits the incorporation of some 3-dimensional important factors in aquatic ecosystems. For instance, water circulation dynamics and wind-driven circulation events alter the movement and distribution of nutrients, plankton and animals [1, 4, 14–16, 35]. Climate change has been shown to alter hydrodynamics in the ocean [66] and could potentially drive changes in DVM and primary productivity in freshwater systems. As such, extensions of our model could expand to 3 dimensions and incorporate water circulation as a driver of DVM dynamics. Freshwater systems are also very spatially heterogeneous with respect to nutrient concentrations [2, 42]. A 3-dimensional extension of our model, including a third dimension of membranes, could include the effects of nutrients for freshwater systems that vary in their trophic state to determine how cultural eutrophication and climate change interact to affect DVM. Ultimately, our model provides a framework for building such extensions for further investigations.

Additionally, our current model represents *Daphnia* predation as a function inversely proportional to water depth. This stationary representation of *Daphnia* predators obviates the dynamics of these fisheries species such as bluegill (*Lepomis macrochirus*) [61]. In this sense, we propose to extend our current model by explicitly modeling groups of *Daphnia* predators as objects that can migrate across the membrane graph, feeding on *Daphnia* and reproducing by egg-laying in a lifecycle akin to that of *Daphnia*. We anticipate that such an extension of our model would change the predictions on *Daphnia* spatial distribution and biomass.

In a broader sense, membrane computing is an exceptional framework to model the dynamics of animal species moving across an area. Membrane graphs provide a natural mechanism to encode spatial regions. In this sense, there exist membrane computing models on population dynamics that use a membrane graph to represent space [13, 18, 21]. However, the usage of a membrane graph to represent a lattice of spatial regions is not common in the literature of membrane computing models in population dynamics, even though it is a widespread practice in agent-based modeling in fisheries [5, 12, 37, 38]. In this sense, we plan to apply membrane computing as a modeling framework for spatially-explicit phenomena in population dynamics in aquatic ecosystems, using membrane grids to represent spatial and other types of regions.

Acknowledgements This work was supported by the Jefferson Project at Lake George, which is a collaboration between Rensselaer Polytechnic Institute, IBM, and The FUND for Lake George. The funding sources had no involvement in the model design, implementation and simulation, the writing of this article, or in the decision to submit this article for publication.

References

1. Abbaspour, K. C., Yang, J., Maximov, I., Siber, R., Bogner, K., Mieleitner, J., et al. (2007). Modelling hydrology and water quality in the pre-alpine/alpine Thur watershed using SWAT. *Journal of Hydrology*, *333*(2–4), 413–430. https://doi.org/10.1016/j.jhydrol.2006.09.014.
2. Allan, M. G., Hamilton, D. P., Trolle, D., Muraoka, K., & McBride, C. (2016). Spatial heterogeneity in geothermally-influenced lakes derived from atmospherically corrected Landsat thermal imagery and three-dimensional hydrodynamic modelling. *International Journal of Applied Earth Observation and Geoinformation*, *50*, 106–116. https://doi.org/10.1016/J.JAG.2016.03.006.
3. Barbuti, R., Bove, P., Milazzo, P., & Pardini, G. (2015). Minimal probabilistic P systems for modelling ecological systems. *Theoretical Computer Science*, *608*(Part 1), 36–56. https://doi.org/10.1016/j.tcs.2015.07.035.
4. Beletsky, D., Schwab, D., Mason, D., Rutherford, E., McCormick, M., Vanderploeg, H., & Janssen, J. (2003). Modeling the transport of larval Yellow Perch in Lake Michigan. In: *Estuarine and coastal modeling* (pp. 439–454). Reston, VA: American Society of Civil Engineers (2004). https://doi.org/10.1061/40734(145)28
5. Berec, L. (2002). Techniques of spatially explicit individual-based models: Construction, simulation, and mean-field analysis. *Ecological Modelling*, *150*(1–2), 55–81. https://doi.org/10.1016/S0304-3800(01)00463-X.
6. Berger, J., Young, J. K., & Berger, K. M. (2008). Protecting migration corridors: Challenges and optimism for Mongolian Saiga. *PLoS Biology*, *6*(7), e165. https://doi.org/10.1371/journal.pbio.0060165.
7. Besozzi, D., Cazzaniga, P., Pescini, D., & Mauri, G. (2008). Modelling metapopulations with stochastic membrane systems. *Biosystems*, *91*(3), 499–514. https://doi.org/10.1016/j.biosystems.2006.12.011.
8. Bollens, S. M., Frost, B. W., & Cordell, J. R. (1994). Chemical, mechanical and visual cues in the vertical migration behavior of the marine planktonic copepod *Acartia hudsonica*. *Journal of Plankton Research*, *16*(5), 555–564. https://doi.org/10.1093/plankt/16.5.555.
9. Boriss, H., & Gabriel, W. (1998). Vertical migration in *Daphnia*: The role of phenotypic plasticity in the migration pattern for competing clones or species. *Oikos*, *83*(1), 129. https://doi.org/10.2307/3546553.
10. Brewer, M. C., Dawidowicz, P., & Dodson, S. I. (1999). Interactive effects of fish kairomone and light on *Daphnia* escape behavior. *Journal of Plankton Research*, *21*(7), 1317–1335. https://doi.org/10.1093/plankt/21.7.1317.
11. Burns, C. W. (1969). Relation between filtering rate, temperature, and body size in four species of Daphnia. *Limnology and Oceanography*, *14*(5), 693–700. https://doi.org/10.4319/lo.1969.14.5.0693.
12. Cao, J., Guan, W., Truesdell, S., Chen, Y., & Tian, S. (2016). An individual-based probabilistic model for simulating fisheries population dynamics. *Aquaculture and Fisheries*, *1*, 34–40. https://doi.org/10.1016/j.aaf.2016.10.001.
13. Cardona, M., Colomer, M. A., Margalida, A., Palau, A., Pérez-Hurtado, I., Pérez-Jiménez, M. J., & Sanuy, D. (2011). A computational modeling for real ecosystems based on P systems. In: *Natural computing* (Vol. 1, pp. 39–53). Springer. https://doi.org/10.1007/s11047-010-9191-3.
14. Cerco, C. F. (1995). Simulation of long-term trends in Chesapeake Bay eutrophication. *Journal of Environmental Engineering*, *121*(4), 298–310. https://doi.org/10.1061/(ASCE)0733-9372(1995)121:4(298).
15. Cerco, C. F., & Meyers, M. (2000). Tributary refinements to Chesapeake Bay Model. *Journal of Environmental Engineering*, *126*(2), 164–174. https://doi.org/10.1061/(ASCE)0733-9372(2000)126:2(164).
16. Chau, K. W., & Jin, H. (1998). Eutrophication model for a Coastal Bay in Hong Kong. *Journal of Environmental Engineering*, *124*(7), 628–638. https://doi.org/10.1061/(ASCE)0733-9372(1998)124:7(628).
17. Ciencialová, L., Csuhaj-Varjú, E., Cienciala, L., & Sosík, P. (2019). P colonies. *Journal of Membrane Computing*, *1*(3), 178–197. https://doi.org/10.1007/s41965-019-00019-w.
18. Colomer, M., Lavín, S., Marco, I., Margalida, A., Pérez-Hurtado, I., Pérez-Jiménez, M., Sanuy, D., Serrano, E., & Valencia-Cabrera, L. (2011). Modeling population growth of *Pyrenean chamois* (*Rupicapra p. pyrenaica*) by using p-systems. In: M. Gheorghe, T. Hinze, G. Păun, G. Rozenberg, A. Salomaa (Eds.) *Membrane Computing, Lecture Notes in Computer Science* (Vol. 6501, pp. 144–159). Berlin: Springer. https://doi.org/10.1007/978-3-642-18123-8_13.
19. Colomer, M. A., Margalida, A., & Pérez-Jiménez, M. J. (2013). Population dynamics P aystem (PDP) models: A standardized protocol for describing and applying novel bio-inspired computing tools. *PLoS ONE*, *8*(4), e60698. https://doi.org/10.1371/journal.pone.0060698.
20. Colomer, M. A., Margalida, A., Sanuy, D., & Pérez-Jiménez, M. J. (2011). A bio-inspired computing model as a new tool for modeling ecosystems: The avian scavengers as a case study. *Ecological Modelling*, *222*(1), 33–47. https://doi.org/10.1016/j.ecolmodel.2010.09.012.
21. Colomer, M. A., Margalida, A., Valencia, L., & Palau, A. (2014). Application of a computational model for complex fluvial ecosystems: The population dynamics of zebra mussel *Dreissena polymorpha* as a case study. *Ecological Complexity*, *20*, 116–126. https://doi.org/10.1016/j.ecocom.2014.09.006.
22. Colomer-Cugat, M. A., García-Quismondo, M., Macías-Ramos, L. F., Martínez-del Amor, M. A., Pérez-Hurtado, I., Pérez-Jiménez, M. J., Riscos-Núñez, A., & Valencia-Cabrera, L. (2014). Membrane system-based models for specifying dynamical population systems (pp. 97–132). Cham: Springer International Publishing. https://doi.org/10.1007/978-3-319-03191-0_4.
23. Cooke, S. L., Williamson, C. E., Leech, D. M., Boeing, W. J., & Torres, L. (2008). Effects of temperature and ultraviolet radiation on diel vertical migration of freshwater crustacean zooplankton. *Canadian Journal of Fisheries and Aquatic Sciences*, *65*(6), 1144–1152. https://doi.org/10.1139/F08-039.
24. Coumou, D., & Rahmstorf, S. (2012). A decade of weather extremes. *Nature Climate Change*, *2*(7), 491. https://doi.org/10.1038/nclimate1452.
25. Dodson, S. (1990). Predicting diel vertical migration of zooplankton. *Limnology and Oceanography*, *35*(5), 1195–1200. https://doi.org/10.4319/lo.1990.35.5.1195.

26. Dodson, S. I., Tollrian, R., & Lampert, W. (1997). *Daphnia* swimming behavior during vertical migration. Tech. Rep. 8. https://academic.oup.com/plankt/article-abstract/19/8/969/1471878.
27. Eiane, K., & Parisi, D. (2001). Towards a robust concept for modelling zooplankton migration. *Sarsia*, *86*(6), 465–475. https://doi.org/10.1080/00364827.2001.10420486.
28. Elert, E. V., & Pohnert, G. (2000). Predator specificity of kairomones in diel vertical migration of Daphnia: a chemical approach. *Oikos*, *88*(1), 119–128. https://doi.org/10.1034/j.1600-0706.2000.880114.x.
29. Fiksen, Ø. (1997). Allocation patterns and diel vertical migration: Modeling the optimal *Daphnia*. *Ecology*, *78*(5), 1446–1456. https://doi.org/10.1890/0012-9658(1997)078[1446:APADVM]2.0.CO;2.
30. Fischer, J. M., Nicolai, J. L., Williamson, C. E., Persaud, A. D., & Lockwood, R. S. (2006). Effects of ultraviolet radiation on diel vertical migration of crustacean zooplankton: An in situ mesocosm experiment. *Hydrobiologia*, *563*(1), 217–224. https://doi.org/10.1007/s10750-005-0007-x.
31. García-Quismondo, M. (2014). Modelling and simulation of real-life phenomena in membrane computing. Ph.D. thesis, Department of Computer Science and Artificial Intelligence. University of Sevilla.
32. García-Quismondo, M., Martínez-del-Amor, M. A., & Pérez-Jiménez, M. J. (2015). Probabilistic guarded P systems, a new formal modelling framework. *Lecture Notes in Computer Science*, *8961*(1), 194–214.
33. García-Quismondo, M., Levin, M., & Lobo, D. (2017). Modeling regenerative processes with membrane computing. *Information Sciences*, *381*, 229–249. https://doi.org/10.1016/j.ins.2016.11.017.
34. García-Quismondo, M., Reed, J. M., Chew, F. S., del Amor, M. A. M., & Pérez-Jiménez, M. J. (2017). Evolutionary response of a native butterfly to concurrent plant invasions: Simulation of population dynamics. *Ecological Modelling*, *360*, 410–424. https://doi.org/10.1016/j.ecolmodel.2017.06.030.
35. Gin, K. Y. H., Zhang, Q. Y., Chan, E. S., & Chou, L. M. (2001). Three-dimensional ecological-eutrophication model for Singapore. *Journal of Environmental Engineering*, *127*(10), 928–937. https://doi.org/10.1061/(ASCE)0733-9372(2001)127:10(928).
36. van Gool, E., & Ringelberg, J. (1997). The effect of accelerations in light increase on the phototactic downward swimming of *Daphnia* and the relevance to diel vertical migration. *Journal of Plankton Research*, *19*(12), 2041–2050. https://doi.org/10.1093/plankt/19.12.2041.
37. Grimm, V. (1999). Ten years of individual-based modelling in ecology: What have we learned and what could we learn in the future? *Ecological Modelling*, *115*(2), 129–148. https://doi.org/10.1016/S0304-3800(98)00188-4.
38. Grimm, V., Wyszomirski, T., Aikman, D., & Uchmański, J. (1999). Individual-based modelling and ecological theory: Synthesis of a workshop. *Ecological Modelling*, *115*(2), 275–282. https://doi.org/10.1016/S0304-3800(98)00186-0.
39. Han, B. P., & Straškraba, M. (2001). Control mechanisms of diel vertical migration: Theoretical assumptions. *Journal of Theoretical Biology*, *210*(3), 305–318. https://doi.org/10.1006/JTBI.2001.2307.
40. Hansson, L. A., & Hylander, S. (2009). Size-structured risk assessments govern *Daphnia* migration. *Proceedings of the Royal Society B: Biological Sciences*, *276*(276), 331–336. https://doi.org/10.1098/rspb.2008.1088.
41. Hays, G. C. (2003). A review of the adaptive significance and ecosystem consequences of zooplankton diel vertical migrations. *Hydrobiologia*, *503*(1–3), 163–170. https://doi.org/10.1023/B:HYDR.0000008476.23617.b0.
42. Hoellein, T. J., Bruesewitz, D. A., & Hamilton, D. P. (2012). Are geothermal streams important sites of nutrient uptake in an agricultural and urbanising landscape (Rotorua, New Zealand)? *Freshwater Biology*, *57*(1), 116–128. https://doi.org/10.1111/j.1365-2427.2011.02702.x.
43. Huntley, B., Collingham, Y. C., Green, R. E., Hilton, G. M., Rahbek, C., & Willis, S. G. (2006). Potential impacts of climatic change upon geographical distributions of birds. *Ibis*, *148*, 8–28. https://doi.org/10.1111/j.1474-919X.2006.00523.x.
44. Hylander, S., Larsson, N., & Hansson, L. A. (2009). Zooplankton vertical migration and plasticity of pigmentation arising from simultaneous UV and predation threats. *Limnology and Oceanography*, *54*(2), 483–491. https://doi.org/10.4319/lo.2009.54.2.0483.
45. Juayong, R. A. B., & Adorna, H. N. (2020). A survey of results on evolution-communication P systems with energy. *Journal of Membrane Computing*, *2*(1), 59–69. https://doi.org/10.1007/s41965-020-00034-2.
46. Kessler, K., & Lampert, W. (2004). Depth distribution of Daphnia in response to a deep-water algal maximum: The effect of body size and temperature gradient. *Freshwater Biology*, *49*(4), 392–401. https://doi.org/10.1111/j.1365-2427.2004.01190.x.
47. Laaksonen, T., Ahola, M., Eeva, T., Väisänen, R., & Lehikoinen, E. (2006). Climate change, migratory connectivity and changes in laying date and clutch size of the pied flycatcher. *Oikos*, *114*(2), 277–290. https://doi.org/10.1111/j.2006.0030-1299.14652.x.
48. Lampert, W. (1989). The adaptive significance of diel vertical migration of zooplankton. *Functional Ecology*, *3*(1), 21. https://doi.org/10.2307/2389671.
49. Leporati, A., Manzoni, L., Mauri, G., Porreca, A. E., & Zandron, C. (2020). Shallow laconic P systems can count. *Journal of Membrane Computing*, *2*(1), 49–58. https://doi.org/10.1007/s41965-020-00032-4.
50. Loose, C. J., & Dawidowicz, P. (1994). Trade-offs in diel vertical migration by zooplankton: The costs of predator avoidance. *Ecology*, *75*(8), 2255. https://doi.org/10.2307/1940881.
51. Morozov, A. Y., Petrovskii, S. V., & Nezlin, N. P. (2007). Towards resolving the paradox of enrichment: The impact of zooplankton vertical migrations on plankton systems stability. *Journal of Theoretical Biology*, *248*(3), 501–511. https://doi.org/10.1016/J.JTBI.2007.05.028.
52. Orellana-Martín, D., Valencia-Cabrera, L., Riscos-Núñez, A., & Pérez-Jiménez, M. J. (2019). Minimal cooperation as a way to achieve the efficiency in cell-like membrane systems. *Journal of Membrane Computing*, *1*(2), 85–92. https://doi.org/10.1007/s41965-018-00004-9.
53. Park, R. A., Clough, J. S., & Wellman, M. C. (2008). AQUATOX: Modeling environmental fate and ecological effects in aquatic ecosystems. *Ecological Modelling*, *213*(1), 1–15. https://doi.org/10.1016/j.ecolmodel.2008.01.015.
54. Pinheiro, J., Bates, D., DebRoy, S., & Sarkar, D. (2017). R Core Team: nlme: Linear and nonlinear mixed effects models. https://cran.r-project.org/package=nlme.
55. Păun, G. (2000). Computing with membranes. *Journal of Computer and System Sciences*, *61*(1), 108–143. https://doi.org/10.1006/jcss.1999.1693.
56. R Core Team. (2017). R: A language and environment for statistical computing. Vienna: R Foundation for Statistical Computing. https://www.r-project.org/.
57. Ramos-Jiliberto, R., & González-Olivares, E. (2000). Relating behavior to population dynamics: A predator-prey metaphysiological model emphasizing zooplankton diel vertical migration as an inducible response. *Ecological Modelling*, *127*(2–3), 221–233. https://doi.org/10.1016/S0304-3800(99)00214-8.
58. Richards, S. A., Possingham, H. P., & Noye, J. (1996). Diel vertical migration: modelling light-mediated mechanisms. *Journal of Plankton Research*, *18*(12), 2199–2222. https://doi.org/10.1093/plankt/18.12.2199.

59. Rinke, K., & Petzoldt, T. (2003). Modelling the effects of temperature and food on individual growth and reproduction of *Daphnia* and their consequences on the population level. *Limnologica - Ecology and Management of Inland Waters*, *33*(4), 293–304. https://doi.org/10.1016/S0075-9511(03)80024-5.
60. Rinke, K., Petzoldt, T. (2008). Individual-based simulation of diel vertical migration of *Daphnia*: A synthesis of proximate and ultimate factors. Limnologica - Ecology and Management of Inland Waters **38**(3-4), 269–285. https://doi.org/10.1016/j.limno.2008.05.006. http://linkinghub.elsevier.com/retrieve/pii/S0075951108000297.
61. Rose, K. C., Williamson, C. E., Fischer, J. M., Connelly, S. J., Olson, M., Tucker, A. J., et al. (2012). The role of ultraviolet radiation and fish in regulating the vertical distribution of *Daphnia*. *Limnology and Oceanography*, *57*(6), 1867–1876. https://doi.org/10.4319/lo.2012.57.6.1867.
62. Ryabov, A. B. (2012). Phytoplankton competition in deep biomass maximum. *Theoretical Ecology*, *5*(3), 373–385. https://doi.org/10.1007/s12080-012-0158-0.
63. Samanta, S., Alquran, M., & Chattopadhyay, J. (2015). Existence and global stability of positive periodic solution of tri-trophic food chain with middle predator migratory in nature. *Applied Mathematical Modelling*, *39*(15), 4285–4299. https://doi.org/10.1016/j.apm.2014.12.044.
64. Samanta, S., & Chattopadhyay, J. (2013). Effect of kairomone on predator-prey dynamics—A delay model. *International Journal of Biomathematics*, *06*(05), 1350035. https://doi.org/10.1142/S1793524513500356.
65. Song, B., Li, K., Orellana-Martín, D., Valencia-Cabrera, L., & Pérez-Jiménez, M. J. (2020). Cell-like P systems with evolutional symport/antiport rules and membrane creation. *Information and Computation*,. https://doi.org/10.1016/j.ic.2020.104542.
66. Sydeman, W. J., García-Reyes, M., Schoeman, D. S., Rykaczewski, R. R., Thompson, S. A., Black, B. A., et al. (2014). Climate change and wind intensification in coastal upwelling ecosystems. *Science*, *345*(6192), 77–80. https://doi.org/10.1126/science.1251635.
67. Visser, M. E., Perdeck, A. C., van Balen, J. H., & Both, C. (2009). Climate change leads to decreasing bird migration distances. *Global Change Biology*, *15*(8), 1859–1865. https://doi.org/10.1111/j.1365-2486.2009.01865.x.
68. Wetzel, R. G. (2001). *Limnology: Lake and river ecosystems*. San Diego: Academic Press.
69. Wilcove, D. S., & Wikelski, M. (2008). Going, going, gone: Is animal migration disappearing. *PLoS Biology*, *6*(7), e188. https://doi.org/10.1371/journal.pbio.0060188.
70. Williamson, C. E., Fischer, J. M., Bollens, S. M., Overholt, E. P., & Breckenridge, J. K. (2011). Toward a more comprehensive theory of zooplankton diel vertical migration: Integrating ultraviolet radiation and water transparency into the biotic paradigm. *Limnology and Oceanography*, *56*(5), 1603–1623. https://doi.org/10.4319/lo.2011.56.5.1603.
71. Williamson, C. E., Zepp, R. G., Lucas, R. M., Madronich, S., Austin, A. T., Ballaré, C. L., et al. (2014). Solar ultraviolet radiation in a changing climate. *Nature Climate Change*, *4*(6), 434–441. https://doi.org/10.1038/nclimate2225.
72. Xu, H., Paerl, H. W., Qin, B., Zhu, G., Hall, N. S., & Wu, Y. (2015). Determining critical nutrient thresholds needed to control harmful cyanobacterial blooms in Eutrophic Lake Taihu, China. *Environmental Science & Technology*, *49*(2), 1051–1059. https://doi.org/10.1021/es503744q.

Manuel García-Quismondo is a computational biologist at One-Three Biotech. His areas of research include computational modeling, bioinformatics, machine learning, population dynamics and high performance computing. He has held fellowships at multiple academic institutions, including the University of Sevilla (Spain), Manchester Metropolitan University (UK), Huazhong University of Science and Technology (China), Tufts University, University of Minnesota, Rutgers University, Smithsonian Institution, Rensselaer Polytechnic Institute and Icahn School of Medicine at Mount Sinai.

William D. Hintz is an assistant professor at the University of Toledo in Ohio, United States. He holds a B.Sc., M.Sc., and Ph.D. in ecology. His current research interests are the interactive effects of multiple stressors on freshwater webs and the conservation of freshwater fish and fisheries.

Matthew S. Schuler is an assistant professor at Montclair State University in New Jersey, United States. He holds a B.Sc., M.Sc., and Ph.D. in ecology. His current research interests include understanding how contaminants disrupt ecological communities and understanding how multiple stressors disrupt aquatic ecosystems.

Rick A. Relyea is the Director of the Darrin Fresh Water Institute at Rensselaer Polytechnic Institute. He also serves as the Director of the Jefferson Project at Lake George, a groundbreaking partnership between Rensselaer, IBM, and the FUND for Lake George. For the Jefferson Project, he leads a team of scientists, engineers, computer scientists, and artists who are using highly advanced science and technology to understand, predict, and

enable resilient ecosystems. Together, the team has built the "Smartest Lake in the World" at Lake George (NY), using an intelligent sensor network, cutting-edge experiments, and advanced computer modeling. The research is currently expanding to other lakes in the region as The Jefferson Project builds the future of freshwater protection. From 1999 to 2014, he was a professor at the University of Pittsburgh, where he also served as the director of the university's field station, the Pymatuning Laboratory of Ecology.